ISSN 1061-8309, Russian Journal of Nondestructive Testing, 2016, Vol. 52, No. 3, pp. 175–183. © Pleiades Publishing, Ltd., 2016.

MAGNETIC AND ELECTROMAGNETIC METHODS

Defects Detection of Gas Pipeline Near the Welds Based on Self Quotient Image and Discrete Cosine Transform[1]

Hyung Min Kim and Doo-Hyun Choi

School of Electronics Engineering, Kyungpook National University, Daegu 702-701, S. Korea

e-mail: dhc@ee.knu.ac.kr

Received May 14, 2015; in final form, August 20, 2015

Abstract—The magnetic flux leakage (MFL) inspection has been widely used in the inline inspection for the evaluation of steel pipelines and plates. In this paper, a defect detection algorithm based on the MFL inspection is proposed for detecting defects near the welds. The defect in this paper means some deformations and deterioration of steel pipes because of corrosions and cracks by humidity and pressure after gas pipes were buried and it doesn't mean bad welding. The MFL signal of the defects near the welds is worse than that of the far-away from the welds and has low signal-to-noise ratio (SNR). In this paper, the MFL signal of the defects near the welds is enhanced by using the Self Quotient Image (SQI) in this paper and the position of the defects is detected after applying the Discrete Cosine Transform (DCT). Experiments are conducted to demonstrate the accuracy of the proposed defect detection algorithm for the artificial defects carved on the pipes at the pipeline simulation facility (PSF) and the results show that the proposed algorithm can successfully detect the position of the defects on the pipes near the welds.

Keywords: MFL inspection, gas pipeline defects, welding region, SQI, DCT

DOI: 10.1134/S1061830916030049

1. INTRODUCTION

Several million kilometers of gas pipelines are buried throughout the world and the running cost of the pipeline inspection has been on the increase in recent years. The defects that originate in the underground gas pipelines can be classified into corrosion, erosion, crack, pinhole, shallow pitting, deep pitting, etc. [1, 2].

Most of the defects on the pipes are formed near the welds and the more the distance from the welds increases, the more the incidence of defects decreases. When new defect-free pipes are buried, the defects near the welds are generally occurred within 2 to 5 years and the defects which are on about 30 cm away from the welds are occurred within 4 to 10 years [2, 3]. Therefore, the periodic pipe inspection is needed at least once per 5 years.

The management of underground gas pipelines is very important for the safe and stable supply of energy but it is difficult to confirm whether a pipe has deterioration or damage because of the pipes' geographical position. There are many nondestructive testing (NDT) technologies for the evaluation of the condition of gas pipelines. Among them, the MFL inspection using the pipeline inspection gauge (PIG) is suitable when considering transporting materials [4–6]. Before the MFL inspection method was developed, most of the defect's detection works had been concentrated on the use of ultrasonic flaw detection as in such works by Bazulin [7], Polikar [8], Robini [9], Abbate [10], etc. But Polikar, Robini, and Abbate had more emphasis on the defect classification than detection. Since then, the defect detection has been studied by many researchers including Afzal [11]. The study of Afzal focused on the de-noising technique and the noise reduction of MFL signals. Qidwai [12] researched on the defect detection and classification using the fuzzy time-frequency defect classifier. Ma [13] has applied the immune radial basis function neural networks (IRBFNN) for the defect detection. The study of Qidwai and Ma mainly detect the defects located on gas pipes which are not near the welds. Zakara [14] tried to simulate MFL signal using FEMM software and Yang [15] studied defect reconstruction problem. Kandoroodi [16] and Chen [17] also tried to detect defects using MFL signal. Kim [18] and Kim [19] tried to detect complex defects based on MFL signal analysis. Recently, high speed implementation of MFL signal is also tried for real time pigging [20]. This paper presents an algorithm based on SQI and DCT for enhancing the defect detection

[1] The article is published in the original.

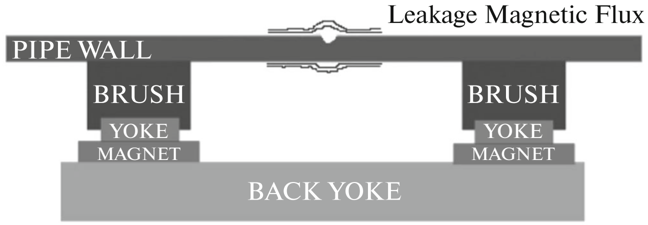

Fig. 1. Magnetic flux leakage pattern due to metal loss [5].

near the welds and analyzes the experimental results. Experimental results are presented to demonstrate the accuracy of the proposed defect detection algorithm for the artificial defects carved on the pipes at the PSF [19].

The remainder of this paper is organized as follows. In Section 2, details of the MFL signal are described. The preprocessing of the MFL signal using SQI is presented and the advantage of the processing is described in Section 3. In Section 4, a defect detection algorithm based on SQI and DCT is proposed. The experimental results are discussed in Section 5 and finally, conclusion is made in Section 6.

2. MFL SIGNAL

When the defect formed on the pipe wall is saturated by permanent magnets in the MFL PIG, magnetic flux leakage is occurred. Usually, the thinner the pipe wall thickness is, the bigger the magnetic flux leakage is. The MFL signal is defined as the magnitude of the leakage magnetic flux measured by a flux-sensitive device such as hall sensors.

Figure 1 shows the MFL PIG which is measuring MFL signals on a defect position [5]. The MFL PIG used in this paper was produced by the research center of a major Korean gas company for gathering the MFL data and it is 30 inches in diameter. 576 hall sensors and 64 eddy-current sensors were mounted on the PIG for the axial, radial, and circumferential direction for considering 3D defect profiles. The MFL data is sampled every 5.23 ms and stored in the data acquisition system (DAS). Traditionally, the measured MFL data is used to estimate the equivalent length, width, and depth of the defects.

Figure 2 shows the MFL signal patterns of the axial, radial and circumferential components, respectively [5]. Actually, the MFL signal of the defect near the welds is worse than that of the far-away location from the welds and has low signal-to-noise ratio (SNR). Welds are inevitably made by welding pipes to make pipelines. In general, welding of pipes is used to overcome the limit of the pipeline length and to connect pipelines with different thickness. If the thickness or the material of pipes is changed, the baseline of the MFL signal is also changed. Also the signal levels itself might be affected [2, 11].

Figure 3 shows the change of the MFL signal when the thickness and the material of the pipe are changed. As shown in Fig. 3, signal is suddenly changed at the welding area. Figure 3a is an A-scan image of axial MFL signals and Fig. 3b is a C-Scan image. Figures 3a and 3b are images of the same region and there is no defect except the welds.

Figure 4a is the A-scan image when the defect exists near the welds. Parts marked with black circle of Fig. 4a are the region where defects are formed. It is difficult to recognize the amplitude of the signal with the naked eye because it's very small. The defect shown in Fig. 4a is formed on a real gas pipe (17.5 mm thickness). The defect is of length 48.9 mm, width 51.2 mm, and depth 3.67 mm and measured precisely by a high-precision measurement tool after excavating the pipes in service. Figure 4b shows the maximum amplitude of the real defect. Note that the leakage flux is bigger as the data goes down from the base level. Figure 4c is the maximum amplitude of an artificial defect (length × width × depth = 52.5 × 52.5 × 3.5 mm) far from the welds. This artificial defect is approximately 1.5 m away from the welds. Even though the size of the defect near the welds is similar to that of the artificial defect, the amplitude of the artificial defect has about 2.04 times bigger than that of the defect near the welds. That is the reason why the leakage flux of the defect near the welds is decreased due to flux that leaks into the welds. Therefore, a new defect detection algorithm is needed when detecting the defect near the welds. In next section, an SQI technique is presented for MFL signal preprocessing.

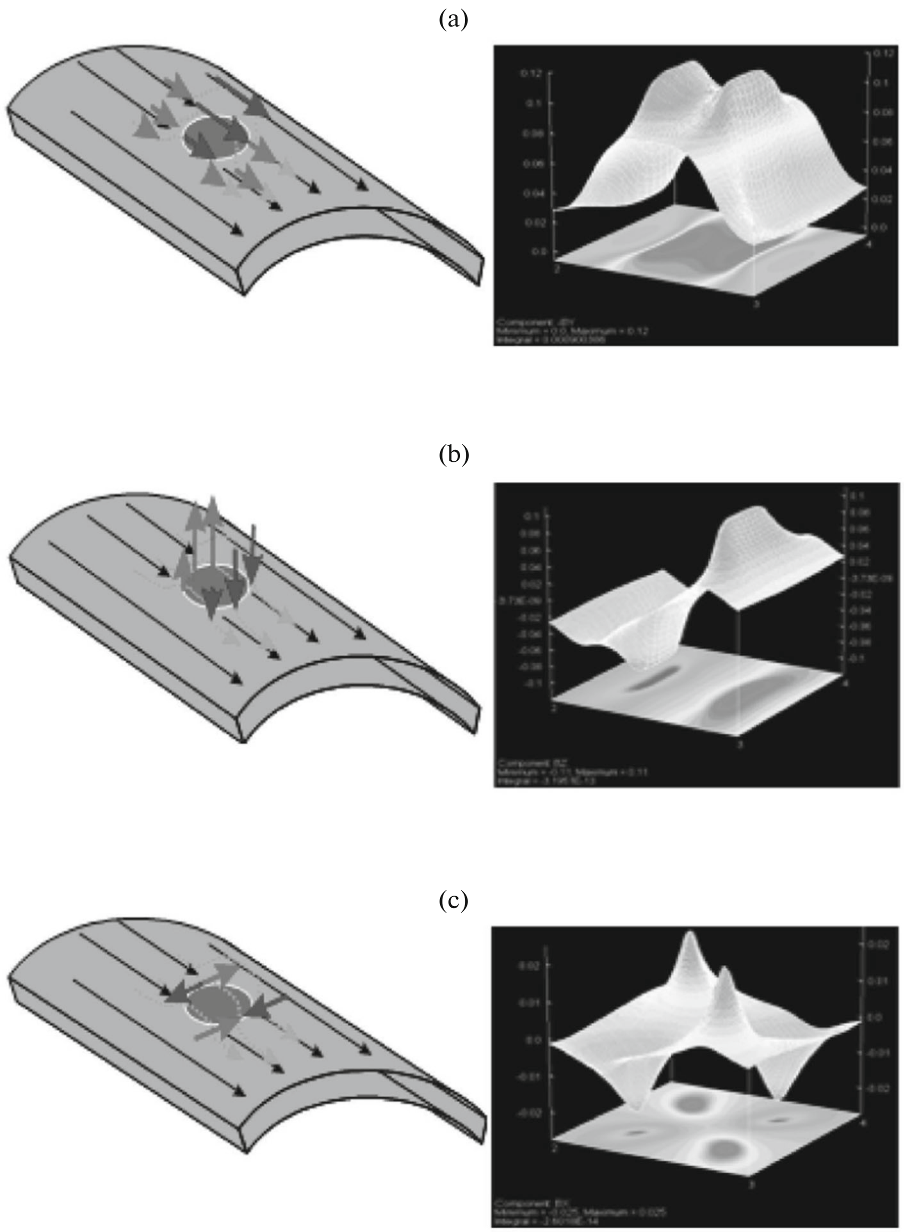

Fig. 2. Signal patterns for each direction [5]: Axial sensor signal (a); Radial sensor signal (b); Circumferential sensor signal (c).

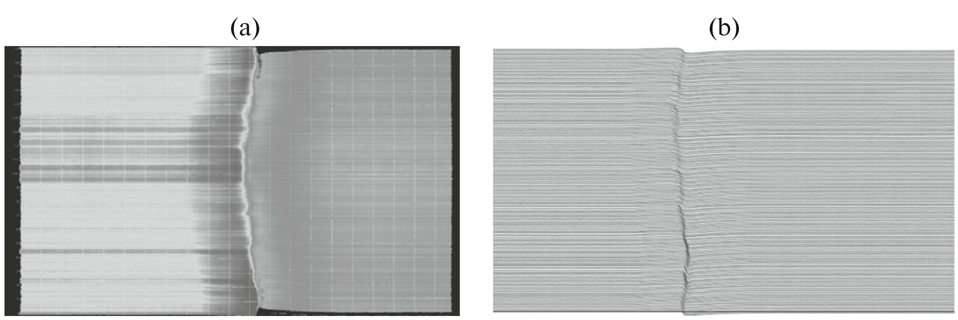

Fig. 3. Axial MFL signals around the welds: A-Scan image (a); C-Scan image (b).

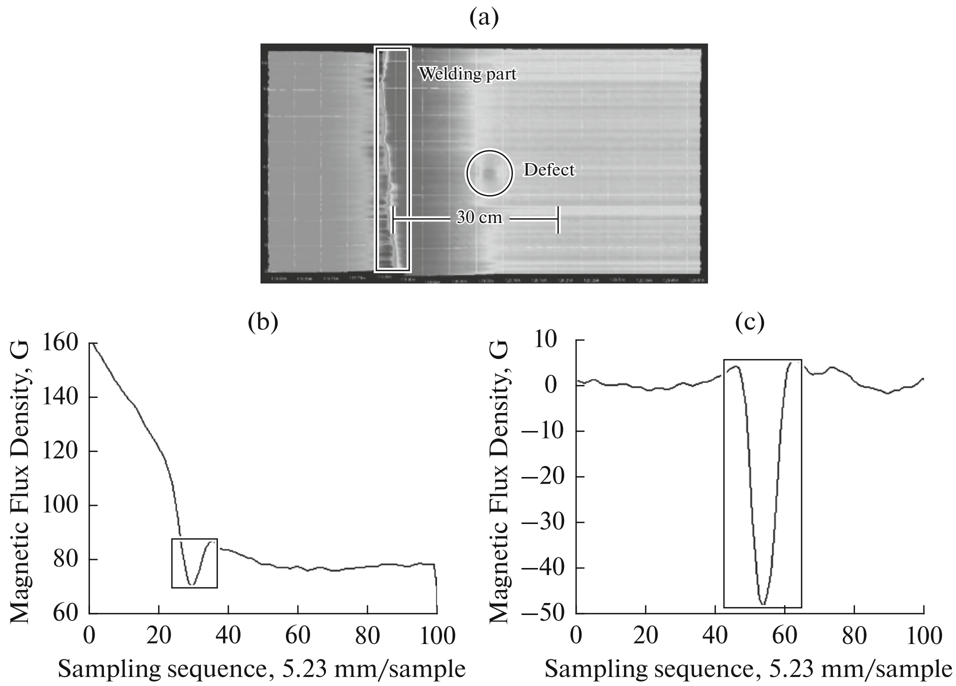

Fig. 4. A-Scan image of a defect near welds and axial MFL signals: A-Scan image of the defect near the welds (a); Axial MFL signal for a defect near the welds (length × width × depth = 48.9 × 51.2 × 3.67 mm) (b); Axial MFL signal for an artificial defect distant to the welds (length × width × depth = 52.5 × 52.5 × 3.5 mm) (c).

3. PREPROCESSING OF MFL SIGNAL USING THE SQI

SQI is a kind of high pass filter (HPF) that separates the signal of low-frequency region based on the information of an original image. As the name implies, SQI is the ratio image between an original image and a low frequency image of the original [21]. In this paper, Gaussian kernel is used as a low-pass filter and the size of the kernel is set to 24 empirically. Equation (1) shows the SQI used in this paper. It is widely used for object recognition like face recognition and vehicle detection under varying lighting condition

$$\hat{I} = \frac{I}{\tilde{I}} = \frac{I}{GI}, \tag{1}$$

where $\hat{I}$—Self Quotient Image; I—original image; $\tilde{I} = GI$—low-pass filtered image; G—Gaussian kernel.

Among the axial MFL signals of five artificial defects carved on the pipes at the PSF, the axial MFL signal of the hall sensors that has maximum amplitude is shown in Fig. 5a. These five defects are above 40 cm away from the welding region. The welding region starts from about 450 sample sequence [5.23 ms/sample] in the figure. As there is a distortion of the signal from about 400 sample sequence due to welds as shown in Fig. 5a, if −145 Gauss may become a threshold for detecting all defects, non-existent defect is detected near about 420 sample sequence due to the welds. Figure 5b is the SQI MFL signal. Unlike Fig. 5a, baseline is aligned to 1 and five defects are correctly detected if under 0.975 becomes a threshold. Figure 5b shows that the SQI MFL signal has high-frequency characteristics of the raw MFL signal and more importantly all the samples have been aligned to the baseline. It’s useful to make a defect detection algorithm.

4. DEFECT DETECTION BASED ON SQI AND DCT

As described in Section 2, three MFL signals exist for three different directions. If all conditions are equal, a radial MFL signal is about 1.3 times bigger than others [5]. But, radial MFL signal is usually polluted by noises such as blooming noise, PIG velocity variation-induced noise, etc., and is also hard to process because a radial MFL signal is affected by the signals due to the welds. For such a reason, proposed defect detection algorithm uses the axial MFL signal. In this paper, 8-point DCT was applied to axial MFL signal and only the 2nd coefficients are used to make a new signal by inverse transforming the coef-

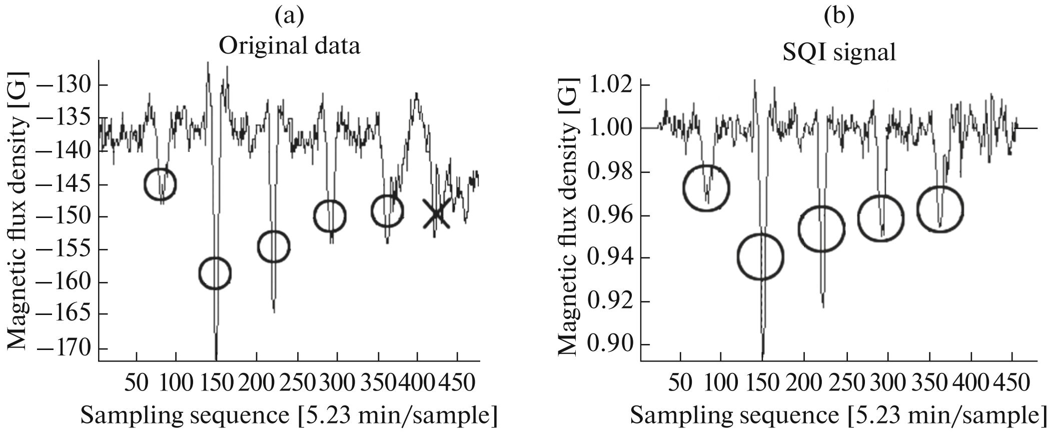

Fig. 5. Raw MFL signals and SQI MFL signals for five artificial defects: MFL signals for five artificial defects (a); SQI-MFL signals for five artificial defects (b).

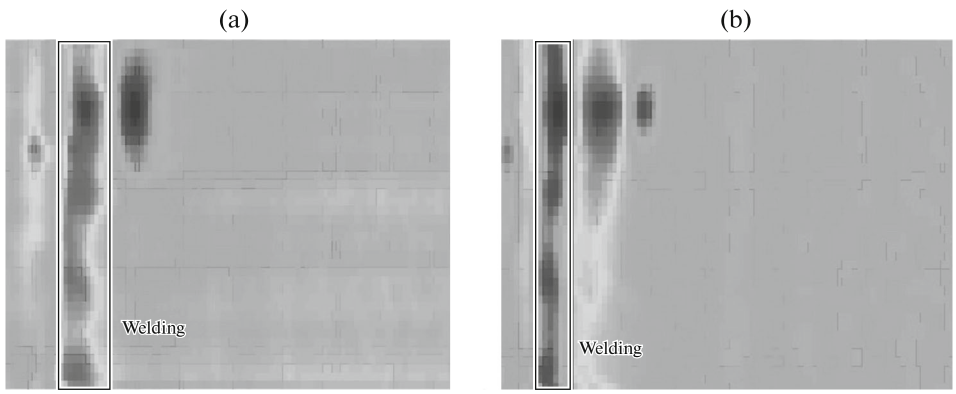

Fig. 6. Pseudo radial MFL signals and raw radial MFL signals for a defect near the welds: Radial MFL signals for a defect near the welds (a); Pseudo radial MFL signals for a defect near the welds (b).

ficients. The basis function of the 2nd coefficients is a cosine function and the coefficient is sensitive to the shape of the axial MFL signal having defects as shown in Fig. 4c. Equation (2) shows the 1-D DCT formula which is used in this paper.

$$F(u) = \frac{C(u)}{2}\sum_{i=0}^{7}\cos\left(\frac{(2i+1)u\pi}{2\times 8}\right)f(i), \tag{2}$$

where $u = 0, 1, \ldots, 7$ and $C(u) = \begin{cases} \frac{\sqrt{2}}{2}, & u = 0 \\ 1, & \text{otherwise} \end{cases}$; $f(i)$—raw MFL signal; $F(u)$—transformed MFL signal.

Figure 6a shows raw radial MFL signals and Fig. 6b does inverse transformed MFL signals from 2nd coefficients of DCT after SQI. Comparing the two signals, the inverse transformed MFL signals are more similar to theoretical radial MFL signals of Fig. 2b. Also raw radial MFL signals are deteriorated by the welds but inverse transformed MFL signals are less deteriorated as shown in the figure.

We call them as a pseudo radial MFL signal. In general, if the radial MFL signals remained intact, defects can be detected by simple thresholding [12]. This paper puts the MFL signal to satisfy both positive Gauss threshold and negative Gauss threshold within a fixed region around welds to the detection criteria of the defects.

Figure 7 summarizes overall block diagram of the proposed algorithm from the signal acquisition to the defect detection.

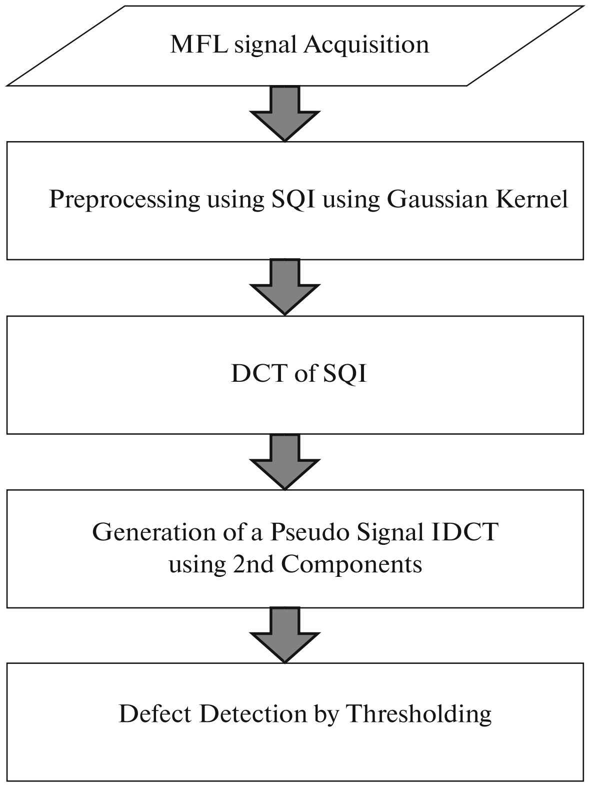

Fig. 7. Block diagram of the proposed algorithm.

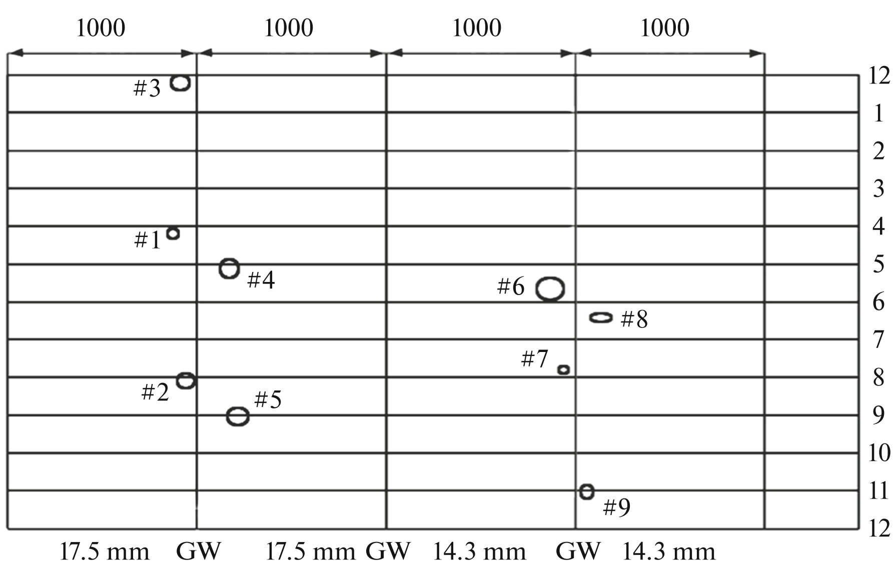

Fig. 8. Distribution of artificial defects near the welds.

5. EXPERIMENTAL RESULTS

This paper uses various artificial defects with different length, width and depth carved on the pipes the PSF to verify the proposed defect detection algorithm around the welding region. Table shows the information of artificial defects carved on the pipes at the PSF.

Figure 8 shows the distribution of the artificial defects near the welds. All the artificial defects are detected correctly by the proposed algorithm without any misdetection and false detection. It means that the application of pseudo signals generated by the corresponding axial signals is a possible strategy to detect defects around the welds. Figure 8 shows the result around two defects, defects 1 and 6.

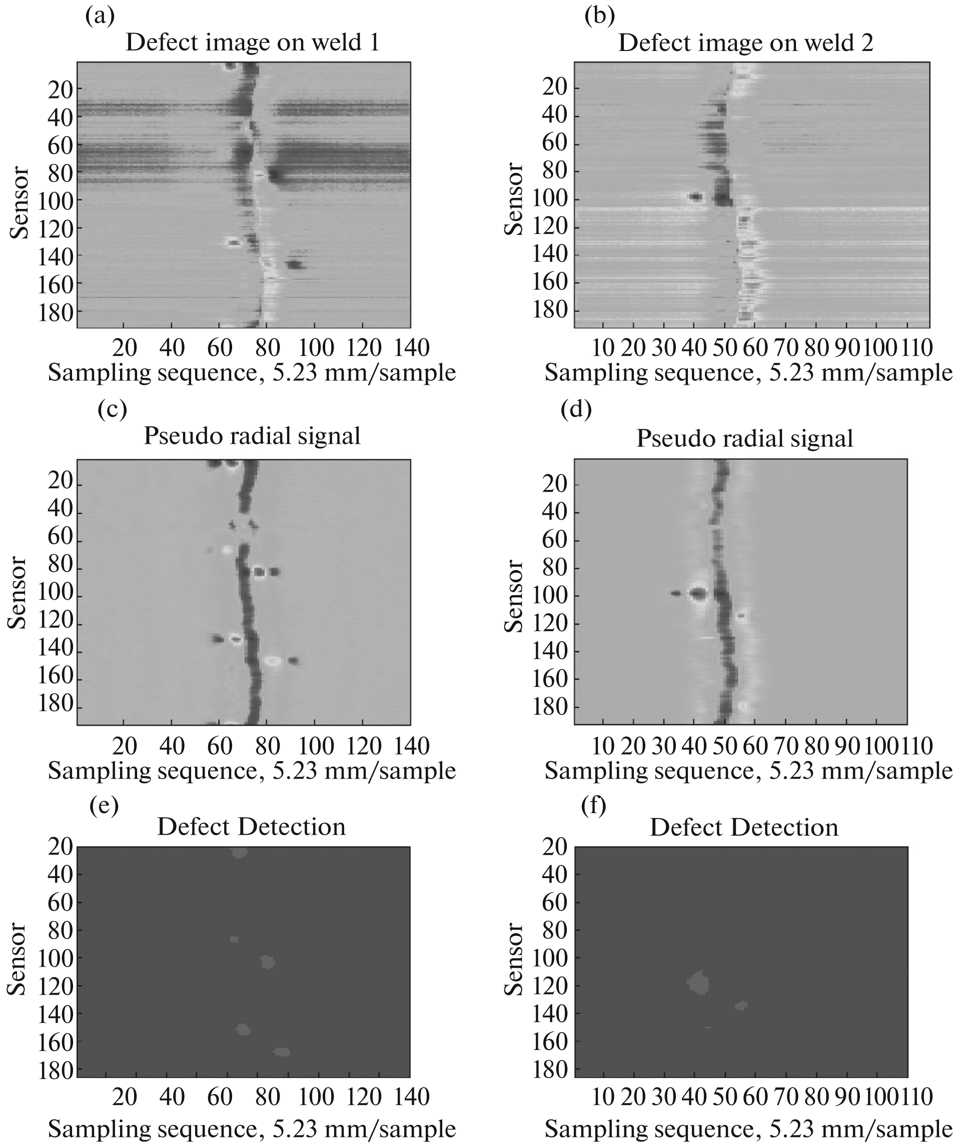

Fig. 9. Pseudo radial signal and defect detection: Radial MFL signals around the defect 1 (a); Radial MFL signals around the defect 6 (b); Pseudo radial MFL signals around the defect 1 (c); Pseudo radial MFL signals around the defect 6 (d); Detection of defects around defect 1 (e); Detection of defects around defect 6 (f).

Figures 9a and 9b is the actual radial MFL signal around defects 1 and 6, respectively. Figures 9c and 9d is the pseudo radial signals generated from the axial signals of the same region of Figs. 9a and 9b, respectively. Some improvement in the point of signals is easily recognized by comparing Fig. 9a with

Artificial defects on the pipes at the pipeline simulation facility

Num.	Clock Position	Defect size ($l \times w \times d$) (cutting angle): mm(°)
1	4	52.5 × 52.5 × 1.75 (45)
2	8	52.5 × 52.5 × 3.5 (45)
3	12	52.5 × 52.5 × 5.25 (45)
4	5	35 × 70 × 3.5 (45)
5	9	70 × 35 × 3.5 (45)
6	6	52.5 × 52.5 × 2.86 (45)
7	8	8.75 × 8.75 × 2.86 (45)
8	6.5	35 × 8.75 × 2.86 (45)
9	11	28.6 × 28.6 × 2.86 (45)

Fig. 9c and Figs. 9b with 9d. Using the signals of Figs. 9c and 9d the final defect detection result near the welds are shown in Figs. 9e and 9f. As shown in Figs. 9e and 9f, all the defects are detected correctly and it is easily found that the pseudo signals for defect detection near the welds is useful by comparing raw radial signals of Figs. 9a and 9b with Figs. 9c and 9d.

6. CONCLUSIONS

In this paper, a defect detection algorithm using SQI and DCT is proposed for detecting defects near the welds. Raw MFL signal from a MFL PIG is noisy and inconsistent bias occurred by PIG velocity, physical environmental conditions, pipe welding, etc. These noise and inconsistency are main obstacles of detecting defects. Proposed algorithm tries to find a solution to reduce the impact of these obstacles.

In this paper, inconsistent bias of MFL signal occurred from various environmental conditions is reduced by SQI and the pseudo radial MFL signals are generated from the axial MFL signals by applying DCT. Experimental results are presented to demonstrate the accuracy of the proposed defect detection algorithm for the artificial defects carved on the pipes at the PSF. It shows that the proposed algorithm can successfully detect the position of defects on the pipes near the welds. The proposed algorithm is simple and high speed algorithms for SQI have also suggested by other research it can be easily applied to PIGs for real time inspection.

REFERENCES

1. Ginzel, R.K. and Kanters, W.A., *Pipeline Corrosion and Cracking and the Associated Calibration Considerations for Same Side Sizing Applications,* Canada, Ontario, Williamsford: Eclipse Scientific Products Inc., 2002, p. 7.
2. Bubenik, T.A., Nestleroth, J.B., Eiber, R.J., and Saffell, B.F., Magnetic flux leakage technology for natural gas pipeline inspection, Gas Research Institute Topical Report, GRI-91/0367, 1992.
3. Nishida, S.I., Failure of pipeline before service, in *Failure Analysis in Engineering Applications,* Butterworth-Heinemann, UK, 1992, pp. 149–157.
4. Sutherland, J. and Clouston, S., Advances in magnetic flux leakage measurement and inspection for metal loss in pipelines, *3rd International Conference on Pipe Rehabilitation and Maintenance,* Abu Dhabi, UAE, 1999.
5. Gwan Soo Park and Eun Sik Park, Improvement of the sensor system in magnetic flux leakage-type nondestructive testing (NDT), *IEEE Trans. Magnetics*, 2002, vol. 38, no. 2, pp. 1277–1280.
6. Slesarev, D.A. and Abakumov, A.A., Data processing and representation in the MFL method for nondestructive testing, *Russ. J. Nondes. Testing*, 2013, vol. 49, no. 9, pp. 493–498.
7. Bazulin, E.G., Reconstruction of images of reflectors using the correlation method at an arbitrary number of reflections of an ultrasonic pulse from the boundary of a test object that consists of regions with different acoustic properties, *Russ. J. Nondes. Testing*, 2014, vol. 50, no. 9, pp. 515–530.
8. Polikar, R., Udpa, L., Udpa, S., and Taylor, T., Frequency invariant classification of ultrasonic weld inspection signals, *IEEE Trans. Ultrasonics, Ferroelectrics Frequency Control*, 1998, vol. 45, pp. 614–625.
9. Robini, M., Magnin, I., Cattin, H., and Baskurt, A., Two dimensional ultrasonic flaw detection based on wavelet packet transform, *IEEE Trans. Ultrasonics, Ferroelectrics Frequency Control*, 1997, vol. 44, pp. 1382–1394.
10. Abbate, A., Koay, J., Frankel, J., Schroeder, S., and Das, P., Signal detection and noise suppression using a wavelet transform signal processor: application to ultrasonic flaw detection, *IEEE Trans. Ultrasonics, Ferroelectrics Frequency Control*, 1997, vol. 44, pp. 14–26.
11. Afzal, M., Polikar, R., Udpa, L., and Udpa, S., Adaptive noise cancellation schemes for magnetic flux leakage signals obtained from gas pipeline inspection, *IEEE Int. Conf. on Acoustics, Speech Signal Process.*, 2001, vol. 6, pp. 3389–3392.
12. Qidwai, U.A., Autonomous corrosion detection in gas pipelines: a hybrid-fuzzy classifier approach using ultrasonic nondestructive evaluation protocols, *IEEE Trans. Ultrasonics, Ferroelectrics Frequency Control*, 2009, vol. 56, no. 12, pp. 2650–2665.
13. Zhongli Ma and Hongda Liu, Pipeline defect detection and sizing basedon MFL data using immune RBF neural networks, *EEE Congress on Evolutionary Computation,* 2007, pp. 3399–3403.
14. Zakaria, Z., Badri Mansor, M.S., Jahidin, A.H., Azlan, M.S.Z., and Rahim, R.A., Simulation of magnetic flux leakage (MFL) analysis using FEMM software, *IEEE Symposium on Industrial Electronics and Applications,* 2010, pp. 481–486.
15. Yang Lijian, Liu Gang, Zhang Guoguang, and Gao Songwei, Oil-gas pipeline magnetic flux leakage testing defect reconstruction based on support vector machine, *Second International Conference on Intelligent Computation Technology and Automation,* 2009, pp. 395–398.

16. Kandroodi, M.R., Araabi, B.N., Ahmadabadi, M.N., Shirani, F., and Bassiri, M.M., Detection of natural gas pipeline defects using magnetic flux leakage measurements, *21st Iranian Conference on Electrical Engineering,* 2013, pp. 1–6.
17. Liang Chen, Xunbo Li, Guangxu Qin, and Qiang Lu, Signal processing of magnetic flux leakage surface flaw inspect in pipeline steel, *Russ. J. Nondes. Testing*, 2008, vol. 44, no. 12, pp. 859–867.
18. Jong-Hwa Kim, Min-Ho Kim, and Doo-Hyun Choi, Analysis and depth estimation of complex defects on the underground gas pipelines, *J. Magnetics*, 2013, vol. 18, no. 2, pp. 202–206.
19. Min-Ho Kim, Effective estimation of weld defect and complex defect through MFL signal, *Ph. D. Thesis,* S. Korea: Kyungpook National University, 2012.
20. Bok-Jin Oh and Doo-Hyun Choi, Implementation of a modified SQI for the preprocessing of magnetic flux leakage signal, *J. Magnetics*, 2013, vol. 18, no. 3, pp. 357–360.
21. Haitao Wang, Stan Z. Li, and Yangsheng Wang, Face recognition under varying lighting conditions using Self Quotient Image, *Proc. IEEE International Conference on automatic Face and Gesture Recognition,* 2004, pp. 819–824.